



# Effect of pore modulating additives-sepiolite and colloidal nano silica-on physical, mechanical and durability properties of lime-based renders

Francesca Stazi · Valeria Corinaldesi · Ylenia Capotondo · Ilaria Porcarelli · Costanzo Di Perna · Marco D'Orazio

Received: 4 August 2021 / Accepted: 5 April 2022  
© The Author(s) 2022

**Abstract** In hot-humid climates, porous external surfaces of the buildings with high water sorption capabilities could contribute to the surface temperatures reduction through the release of latent heat by evaporative cooling. On the other hand, compact and low permeable finishing materials could have mechanical and durability benefits respect to the underlying supports, for example reducing the permeability to degrading agents. In this paper, the properties of lime base coat renders with pore modulating additives (sepiolite and colloidal nano silica) have been surveyed to evaluate their effectiveness in water

absorption, thermal performance, and the fulfilment of mechanical requirements for the application on the external side of the walls. A traditional lime-sand formulation was taken as reference. After preliminary tests on workability and shrinkage, the optimal mix designs were selected and the samples were subjected to several mechanical and thermo-hygrometric tests, before and after accelerated aging. The results allowed demonstrating that the use of sepiolite in substitution of sand, enhances the render ductility, thermal resistance and water uptake but worsens its mechanical stability, increasing the shrinkage effects and slightly reducing the ultimate strength values. The addition of colloidal nano silica, either to lime-sepiolite or to lime-sand renders, fails to produce any improvement in their either physical or mechanical behavior. Mixed formulations (lime-sand with sepiolite and nano silica) behave as simple lime-sand solutions, showing optimal compressive and flexural strength but reduced water uptake capabilities. This demonstrates that the presence of sand prevails in the performance of the render, and that the adoption of other additives doesn't worth the cost for the benefit presented.

---

F. Stazi (✉) · V. Corinaldesi · Y. Capotondo · I. Porcarelli

Dipartimento di Scienza e Ingegneria della Materia, dell'Ambiente ed Urbanistica (SIMAU), Università Politecnica delle Marche, Via Brecce Bianche, 60131 Ancona, Italy  
e-mail: f.stazi@univpm.it

V. Corinaldesi  
e-mail: v.corinaldesi@univpm.it

C. Di Perna  
Dipartimento di Ingegneria Industriale e Scienze Matematiche, Università Politecnica delle Marche, Via Brecce Bianche, 60131 Ancona, Italy  
e-mail: c.diperna@univpm.it

M. D'Orazio  
Dipartimento di Ingegneria Civile, Edile e Architettura (DICEA), Università Politecnica delle Marche, Via Brecce Bianche, 60131 Ancona, Italy  
e-mail: m.dorazio@univpm.it

**Keywords** Lime render · Sepiolite · Moisture sorption · Colloidal nanosilica · Render performance



## 1 Introduction

The adoption of highly porous materials on external building surfaces could contribute to envelope thermal behavior optimization and external overheating mitigation through the maximization of two effects: one is the cooling effect due to water absorption and subsequent evaporation [1]; the other is the reduction of daily stored heat since porous matrices typically show low conductivity (even more reduced when water absorption takes place) and low thermal capacity [2]. In the last few years, there has been extensive research (i.e. [3, 4]) on the use of porous materials for external building surfaces, to promote the evaporative cooling. According to this method, the retained water in the material pores evaporates, and the component surface temperature is reduced due to the release of latent heat [5]. Therefore, the urban temperatures and the crossing heat flux through the building envelope are reduced and the degradation of construction materials is slowed down [6].

Most of the hi-tech materials specifically tailored to adsorb water (i.e. porous pillared heterostructures, mesoporous molecular sieves, etc.), are laboratory prototypes realized in very small quantities due to structure complexity [7]. Thence, the studies regarding building evaporation cooling are mainly focused on natural porous materials with high water uptake capacity, more suitable for large-scale applications on building surfaces. In such materials, the cooling effect due to the release of latent heat is much faster than that of bulk water due to the increased evaporation area provided by the pores.

Recently, the evaporative cooling principle was applied to moisture sorption on highly hydrophilic natural sepiolite. This material exhibits high water sorption capability and fulfills the compatibility requirements for conservation and restoration of historic masonry supports [8, 9]. Sepiolite is a clay mineral of fibrous morphology with fine microporous channels running parallel to the length of the fibers. Its fibrous composition and the small channels are responsible for its outstanding adsorption properties [10]. Since the water adsorption isotherm of sepiolite shows a large increase in uptake at high relative humidity, this material is suitable as humidity controller in environments characterized by high RHs or as absorber of nighttime moisture [11, 12]. Thence, it's able to lower the temperatures of the external surface

of the building (through the evaporation of water) under irradiation in the following daylight hours [5].

Liquid water is absorbed by capillarity and the bundles of agglomerate needle-like structures form a randomly intermeshed network of fibers that entraps it [10]. The evaluation of water uptake by capillarity could be a preliminary indication of its hygric properties and the evaporative cooling potential [13].

As regards the influence of sepiolite addition on the thermal behavior of renders, in general it can be stated that the evaporation process occurring on a porous surface could produce a significant thermal insulation effect [14]. Some authors also highlighted that porous additives, such as metakaolin admixtures, lower the final thermal conductivity for the increased porosity of the matrix [15]. Other additives, such as waste rubber particles [16] and aerogel granules [17], have been demonstrated to have a beneficial effect on the thermal conductivity of the base materials. Differently, when sand is incorporated into lime based materials, thermal conductivity rises significantly for the density increase [17].

The main drawback of adopting additives intended to improve the hygric properties of a rendering material is the increase of water required to achieve the desired workability, that could cause reduced mechanical performance.

The effect of the addition of sepiolite on the mechanical strength of surface finishing formulations was surveyed for repairing lime–sand based mortars [18] and cement composites [19]. Both studies demonstrated that it has a very positive influence on flexural and compressive strength values, especially at later ages of curing. This result was attributed to the modification of the rheology of the mortar and the consequent formation of a network structure within the main matrix. The sepiolite fibers, characterized by small length and acicular morphology with needle-shaped particles, promote the interlocking of mortar components, resulting in improved mechanical behavior [8]. Other authors [20] confirmed that, even at the varying of the temperature, the use of sepiolite as a binding material with hydraulic lime doesn't have an adverse effect on the mechanical properties of mortar. All the studies regarded the addition of sepiolite on the initial sand-based formulation rather than its substitution in place of sand, so that the mechanical improvement can also be attributed to the natural increase in density.



Among additives with recognized capabilities in the improvement of pores structure, nano silica has been extensively surveyed for concrete matrices. Indeed it has been demonstrated to greatly enhance the performance of cement composites for the refinement of pore structure [21]. Pore diameters of concretes shift to smaller sizes and fall in the range of few-harm pore. [22] Transport of both water and chloride ions in cement is hindered by the addition of colloidal nano silica [23], attributed to the more tortuous pathway, lower porosity and smaller pore size. This determines lower permeability and an improved durability of the component [24, 25].

Moreover, colloidal nano silica can accelerate the rate of cement hydration due to the nucleating effects and has outstanding binding capacity thanks to a pozzolanic reaction [26, 27]. Some authors suggested the use of silica based consolidating additions in thin coatings as strengthening technique for unreinforced masonries [28] in stones or specific types of mortar, particularly earthen mortars [29].

In recent years, there is a renewed interest toward the application of lime renders for the repair of historic buildings [30], due to recognition of drawbacks of Portland cement mortars, namely brittleness, high strength, and a thermal expansion coefficient very higher than lime mortars and most types of brick and stone. Moreover, the low porosity, might determine the deposition of salts in adjacent stones or bricks and the creation of efflorescence. Lime mortar, on the other hand, has a low efflorescence potential due to its relatively high chemical purity [31]. The use of additives able to increase porosity or refine the pore structure could have positive effects on water harvesting capability on one hand and on the permeability reduction to degrading agents on the other hand, with benefits on durability and on the protection of underlying substrates [32, 33], for example historic walls in cob or rammed earth.

In summary, natural porous plasters characterized by unique adsorption properties have aroused great interest, as they are able to promote durability in conservation works [31] and because they represent an economically advantageous solution to improve the evaporative cooling of external surfaces, acting as water reserves [8]. Various authors demonstrated that sepiolite renders are suitable for this purpose.

On the other hand, nanoscale fillers for pore refining, such as silica nanoparticles, have been

successfully incorporated as consolidating elements into cementitious materials demonstrating numerous benefits [39], such as excellent resistance to thermal cracking due to low heat of hydration, an improvement in mechanical strength and durability thanks to the reduction of permeability to external agents [40]. Colloidal nano silica was found to be more convenient in place of dry powder because of its more dispersive nature and reduced segregation [34].

The studies regarding pore modulating fillers are generally focused a single additive, for example sepiolite or nano silica, and one single aspect, for example either the analysis of the high temperature effects on the renders [20], or the verification of the structural / mechanical properties [8, 19], or the maximization of the evaporative cooling and moisture buffering effect ([5, 35]). At the authors' knowledge there are only few studies in literature dealing with the multidisciplinary evaluation of the effect of porosity tuning additives on mechanical, hygroscopic, thermal performance, and durability. Moreover commonly the authors analyzed the sepiolite as adjunctive additive rather than as a substitute for sand (i.e. [8]).

This paper aims at identifying the effect of two different pore modulating additives, namely sepiolite and colloidal nano silica, on the physical, mechanical and durability properties of lime-based renders.

The method involved experimental tests on several render compositions: lime-sand traditional render (reference); lime-sepiolite render (by replacing the sand with sepiolite); mixed lime-sand-sepiolite render; addition of colloidal nano silica in all the previous formulations.

The tests included workability, shrinkage, bulk mass, water uptake, thermal conductivity, and mechanical performance. The same tests were repeated after accelerated aging.

## 2 Materials

The reference lime-sand render consists of hydraulic lime (COLACEM manufacturer, EN 15368 HB 3.0 in powder form), used as a binder material, and a dry siliceous natural sand from river Po, used as aggregate.

An aggregate to binder ratio for the base formulation was fixed at 3:1 by volume. The necessary water amount was obtained in relation to required consistency (i.e. flow table values around 130 mm). The lime

was weighed before and after drying in an oven to remove the water content. The sand, conforming to BS EN 196-1 and ISO 679: 2009, comprises particles that are generally isometric and rounded in shape, with size ranging between 0.25 and 1 mm. The nominal bulk density of the sand falls within the range of 1.4–1.6 g/cm<sup>3</sup>, its specific density is equal to 2.63 g/cm<sup>3</sup>. The lime and sand were prepared using a paddle mixer for a minimum of twenty minutes to ensure that the formulation was suitably workable.

The lime–sepiolite renders were realized both in combination with sand (by replacing 50% of sand volume) and without sand (by fully replacing sand at 100%). A fine sepiolite powder, consisting in hydrated magnesium silicate, with grain size in the range 0.15–3.00 mm (mainly among 0.25–0.5 mm), was adopted (ICEA manufacturer). The recipes were all prepared with the same dosage of lime (Table 1). Due to the lower density of sepiolite with respect to sand, 2.10 g/cm<sup>3</sup> and 2.63 g/cm<sup>3</sup> respectively, the amount of sepiolite fully replacing sand was 750 g instead of 1320 g of sand, while it was dosed at 375 g in combination with 660 g of sand for the mixtures with 50–50% volume proportion of the two aggregate fractions.

Since the use of sepiolite required additional water for workability, with a consequent reduction in compressive strength values, a superplasticizer was added in all the sepiolite-based renders to reduce the water amount and, consequently, to limit the worsening of compressive strength values of the hardened renders. In the case of 100% sepiolite (SEP and SEP\_SC samples), an extra amount of water has been added to guarantee the same fresh consistency class, while in the case of 50% replacement (SAND\_SEP and SAND\_SEP\_SC samples), the only superplasticizer addition at higher dosage (180 g instead of 40 g) was sufficient without adjunctive water.

The superplasticizer was a water solution of naphthalene with a density of 1.2 g/cm<sup>3</sup>, (Mapei Mapefluid N200).

The lime and sepiolite were prepared using a paddle mixer for a minimum of twenty minutes to ensure the renders workability. The water and plasticizer dosages needed to achieve the desired workability and final consistency were provided by the flow table test on two truncated conical specimens for each formulation.

Colloidal nano-silica (SC) supplied by Spray-Lock Concrete Protection, LLC (SCP 1000) was added in both sand and sepiolite samples at the same dosage of 6 g per liter of render. Colloidal nano silica contains 72% solid particles in water solution and has a density of 1.3 g/mL. The specific surface area of nano-silica is 122 m<sup>2</sup>/g. SiO<sub>2</sub> content is 99.8%. An analytical transmission electron microscope (TEM) equipped with diffraction facilities was used to investigate the structure of colloidal nano silica adopted in the present study. Figure 1 reports one of the obtained TEM images that shows the morphology of nano silica particles. The image reveals regular, non-aggregated spherical nanoparticles. The average particles diameter was found to be equal to 10 nm.

The selected mixing ratio of the renders are reported in Table 1.

### 3 Methods

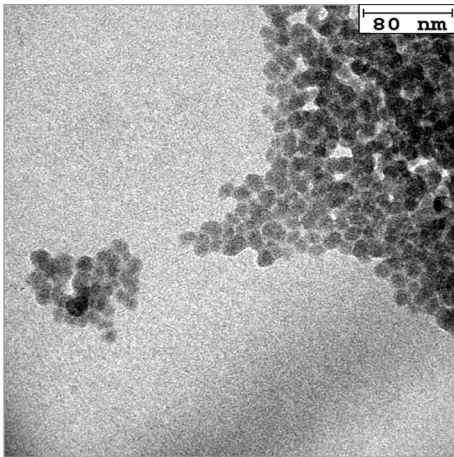
#### 3.1 Consistency and dry bulk density changes

The consistency of each plaster formulation was determined using a flow table test according to EN 1015-3 on two standard cones ( $h = 60$  mm, base diameter = 100 mm, top diameter = 70 mm). The resulting increase in average base diameter of the sample after deformation under its own weight was measured and expressed as a percentage of the original

**Table 1** Renders formulation (ingredients dosage expressed in g for liter of render)

Samples	Lime	Sand	Sepiolite	Water	Superplasticizer	Colloidal nanosilica
SAND	480	1320	–	260	–	–
SAND_SC	480	1320	–	260	–	6
SEP	480	–	750	1260	40	–
SEP_SC	480	–	750	1260	40	6
SAND_SEP	480	660	375	260	180	–
SAND_SEP_SC	480	660	375	260	180	6





**Fig.1** TEM image: morphology of colloidal nano silica particles (SC)

base diameter. The consistency was considered appropriate for increases values lower than 10%. Moreover, the target flow value of the recipes was fixed at  $120 \pm 10$  mm, to secure appropriate on-site workability.

The dry bulk density of hardened mortars was determined on specimens dried at  $(60 \pm 5)$  °C until constant mass, according to EN 1015-10:2007. Three specimens with dimensions 160 mm  $\times$  40 mm  $\times$  40 mm for each composition were tested. The shrinkage was evaluated as the percentage volume reduction of prismatic samples after 28 days of curing.

### 3.2 Pore morphology

Porosity, pore sizes and pore volume measurements were carried out on all samples by a mercury intrusion porosimeter (Pascal 140-240, ThermoFisher). A contact angle of 140.0°, a Hg surface tension of 0.48 N/m and a pressure ranging from 0 to 200 MPa were adopted. The tests were done on small samples of approximately 1.5 g of mass.

### 3.3 Microstructure

A scanning electron microscope SEM (Model: VEGA) was used to examine the microstructure and morphology of the six formulations at 28 days of curing and after the ageing treatment. The samples were obtained from the fragments of the specimens previously subjected to the mechanical tests. The

fragments were inserted into a metal sample holder and fixed to it with a carbon-based glue because of irregular shapes. Subsequently they were covered with a veil of carbon and gold to avoid the accumulation of electrostatic charge on the surface. The beam of electrons accelerated to an energy up to 30 keV.

A study of the microstructure of the rough fractured surfaces was undertaken to directly visualize the structural components of the mortar [36] and to highlight possible fracture mechanisms introduced by increased porosity and aggregates from the morphological analysis of matrix–fibre interface.

### 3.4 Water uptake by capillarity

Three 40 mm  $\times$  40 mm  $\times$  160 mm specimens were prepared for water content test and cured in a climate chamber at a constant temperature of  $20 \pm 2$  °C and relative humidity of  $65 \pm 5\%$  as specified in EN 1015-11:1999. During the first week, since the excessive exposure of the specimen to ambient atmospheric conditions may result in a premature drying and cracking causing a significant reduction in strength values, a high level of humidity of the specimens was maintained by covering them with a thin plastic wrap. Then the specimens were cured in the molds for a further week to allow them to achieve sufficient compactness to facilitate demolding.

The water capillary coefficient was determined according to EN 1015-18:2002. The lateral surfaces of the half specimens ( $69 \pm 1$  mm long) were wrapped in polyethylene film. The prismatic specimens were dried to a constant mass, and then one face of the specimen was immersed in 5–10 mm of water for a specific interval and calculated in mass. The mass gain at 10 and 90 min and the water absorption coefficient were determined according to the standard.

### 3.5 Thermal conductivity

One flat 400 mm  $\times$  400 mm  $\times$  40 mm specimen was realized for the thermal conductivity test and cured as described in Sect. 3.4. Thermal conductivity measurements were obtained using the heat flow meter method described in standard EN 12667:2001 for materials characterized by medium and high thermal resistance. The test system is composed of a box of thick insulating material to ensure an adiabatic test zone with respect to the external environment. A



unidirectional constant and uniform density of heat flow rate was generated by adopting a hot and a cold plate, respectively at 30 and 10 °C, connected to thermostatically—controlled water baths. Temperature probes and flowmeters on both sides of the sample were applied to measure respectively the thermal gradient and the crossing thermal flux ( $q$ ).

### 3.6 Mechanical performance

Three specimens with dimensions 40 mm × 40 mm × 160 mm were prepared and stored in a climate chamber regulated at a constant temperature of 20 ± 2 °C and relative humidity of 65% ± 5% as specified in standard EN 1015-11:1999. The samples were cured as explained in Sect. 3.4. Mechanical strength testing was performed at 28 days of curing with a 200 kN load cell.

The flexural strength was determined by three-point loading of the hardened mortar specimens to failure. The maximal force ( $F$ , N) was measured and the flexural strength ( $\sigma_f$ , N mm<sup>-2</sup>) was calculated as:

$$\sigma_f = 1.5 \frac{F \cdot l}{b \cdot d^2} \quad (1)$$

$F$  (N) is the maximum load applied to the specimen.

$l$  (mm) is the distance between the supports.

$b$  (mm) is the width of the specimen.

$d$  (mm) is the depth of the specimen.

The compressive strength of the mortar was determined on the two portions obtained from the flexural strength test according to BS EN 1015-11. The Young's modulus was determined by obtaining the slope of the near-linear portion of the stress–strain average curve, between approximately 30 and 50% of the ultimate stress as in [37].

The adhesive strength of the formulations was evaluated according to UNI EN 1015-12:2016. The fresh mortar mix was applied to the substrate in raw earth to create five circular specimens with a diameter of approximately 50 mm. Circular rings in stainless steel with an internal diameter of 50 mm and height of 20 mm were used to engrave the fresh render and give it a circular shape. When the mortar was sufficiently hard, the specimens were enclosed within a polyethylene bag at a temperature of 20 °C (± 2 °C) for 7 days. The specimens were stored in air at a constant temperature of 20 °C (± 2 °C) and relative humidity of (65 ± 5) % for further 21 days. After 28 days of

curing, the pull-heads were glued with the adhesive on the test areas. Using the testing machine, the tensile load was applied perpendicularly to the test area.

The adhesive strength (N/mm<sup>2</sup>) was calculated through the following formula:

$$f_u = F_u/A \quad (2)$$

$F_u$  (N) is the maximum load applied to the specimen.

$A$  (mm<sup>2</sup>) is the area of the specimen.

### 3.7 Ageing treatment

The artificial aging was realized following UNI EN ISO 14147:2005, to simulate an aggressive environment with high content of sodium chloride, typical of the climatic Mediterranean context.

Each cycle provided salt fog application for 4 h, the subsequent exposure of the specimens to a hot humid environment for 8 h, following the procedure adopted in [38].

The NaCl: H<sub>2</sub>O solution concentration was 10%. The aging step consisted of 60 cycles, for a total of 42 600 min (30 days). Each cycle included 240 min under salt spray environment (Temperature of 35 ± 5 °C and RH 95%) and 470 min under hot humid environment (Temperature of 35 ± 5 °C and RH 95%). After the cycles the samples were dried at constant temperature of 70 °C until reaching a constant mass and then cooled at environmental temperature before realizing the tests.

## 4 Results

### 4.1 Consistency and dry bulk density


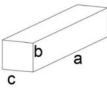
The consistency of fresh formulations was determined through the table test obtained by averaging the base diameter data on two samples for each render formulation. The data are reported in Table 2.

Fresh mortars with sand achieved the best workability than other mortars due to the higher amount of water.

Either the substitution of sand with sepiolite (SEP sample) or the simple addition of sepiolite to the sand (SAND\_SEP) determined a flow value decrease. Other authors obtained similar values for formulations with



**Table 2** Flow test, volume reduction and dry bulk density

Formulation						Dry Bulk density	
	Flow (mm)	$\Delta D$ (%) <sup>*</sup>	$\Delta a$ (mm)	$\Delta b$ (mm)	$\Delta c$ (mm)	At 28 days (g/cm <sup>3</sup> )	After aging treatment (g/cm <sup>3</sup> )
SAND	129	2.3	0	0	0	1.61	1.69
SAND_SC	120	0	0	0	0	1.61	1.66
SEP	120	0.4	8.2 (− 5%) <sup>**</sup>	1.7 (− 1%)	2 (− 1%)	0.82	0.96
SEP_SC	109	0.9	8 (− 5%)	2 (− 1.3%)	2.5 (− 2%)	0.84	0.88
SAND_SEP	111	0	2.5 (− 1.6%)	0	0	1.49	1.49
SAND_SEP_SC	126	0.8	2.5 (− 2%)	0	0	1.50	1.50

\*Average increase (%) of base diameters. This value should be lower than 10%.

\*\*Results in round brackets indicate the relative deformation.

sepiolite additives [8] or other types of additives in substitution to sand [39].

The reason behind this flow reduction might be the structure of small-powdered sepiolite that entraps water thus obstructing the water movement through the fresh mortars. The lowest workability was observed in SEP\_SC since the colloidal nano silica activated a pozzolanic reaction and a change in porosity [40].

The sizes of hardened samples were measured after 28 days of curing to identify possible reductions respect to the reference formulation, on the 3 axes (see Table 2  $\Delta a$ ,  $\Delta b$  and  $\Delta c$ ). The overall volume reduction percentage was calculated and reported in Fig. 2a. SEP and SEP\_SC showed the greatest deformation, in the former case for high water sorption rates of sepiolite, in the latter for the increase of the water demand due to the pozzolanic reaction of nano silica.

The analysis of bulk density of the hardened mortars showed similar low values in sepiolite-based samples (SEP, SEP\_SC), while the density was significantly higher with the use of sand (Table 2 and Fig. 2b). After aging the density slightly increased in SAND and SEP formulations, even with colloidal nano-silica (SC) additions. The use of mixed formulations (SAND-SEP, SAND\_SEP\_SC) achieved the better dimensional stability, showing no density changes. Only SEP and SEP\_SC formulations can be

classified as lightweight mortars having a dry hardened density of less than 1300 kg/m<sup>3</sup>.

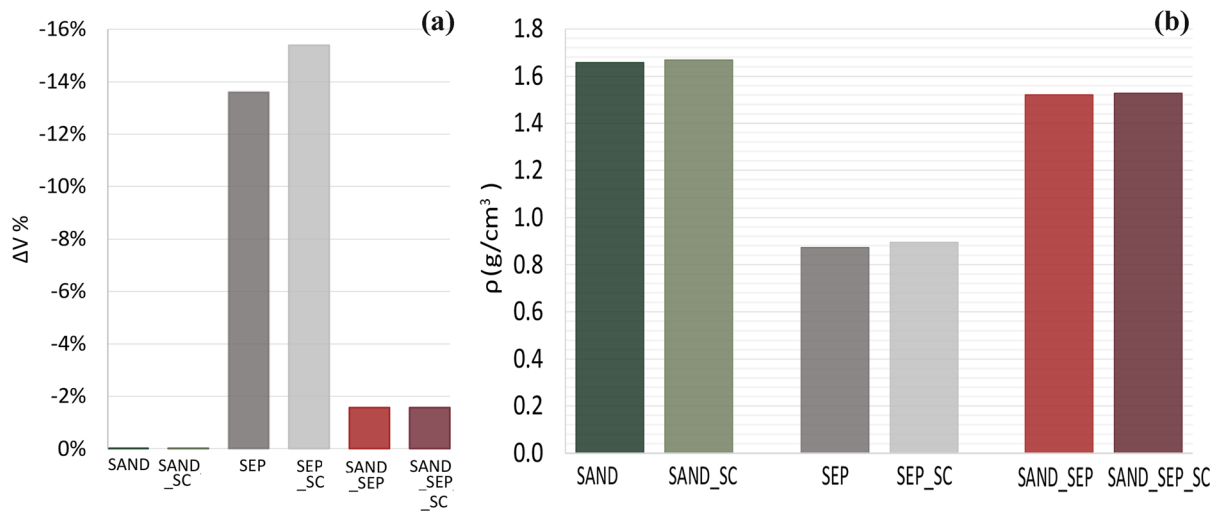
#### 4.2 Pore distribution

Figure 3 reports the results of the porosimeter analysis. The renders with sepiolite (SEP) are characterized by the highest porosity, recording doubled values of accessible porosity compared to reference sand-based plaster and a significant increase of macropores. The presence of sand in mixed solutions had the effect of reducing the porosity increase due to sepiolite. The addition of colloidal nano silica (samples with SC abbreviation) had not significant effects on the accessible porosity (Table 3), but caused an increase in pore average diameter, shifting the morphology towards macro pores.

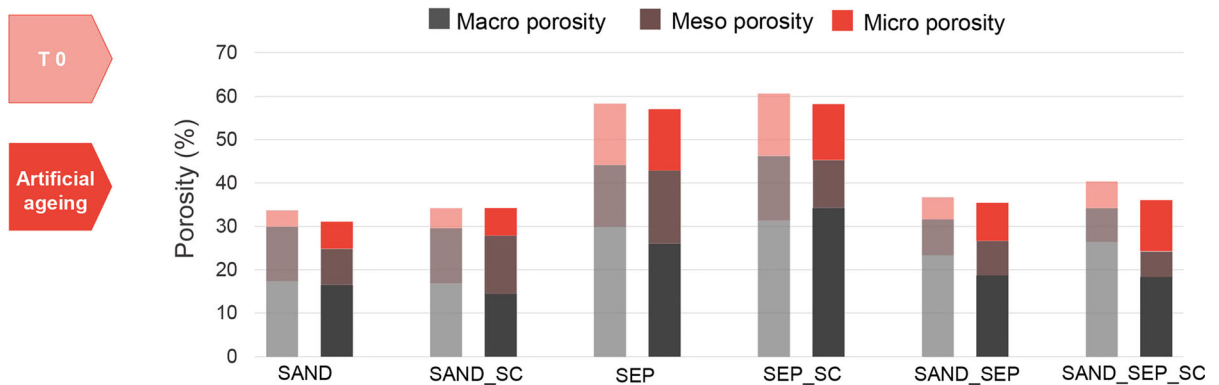
The aging treatment (darker histograms in Fig. 3) for all the formulations reduced the accessible porosity, with the highest impact in SAND-SEP\_SC (see Table 3). Here the ageing determined a refinement of pore structure, shifting the morphology from mainly macro-sized pores to a more homogeneous distribution with a greater micropores quote.

In general, higher porosity was maintained by all the formulations with sepiolite additions.

The addition of colloidal nano silica (SAND\_SC, SEP\_SC, SAND\_SEP\_SC) increased the porosity in all the cases.



**Fig. 2** **a** Total volume reduction percentage at 28 days of curing; **b** density of the samples at 28 days of curing



**Fig.3** Mercury intrusion porosimetry results for unaged mortars (on the left) and aged ones (on the right)

### 4.3 Microstructure

The electron microscope images of SAND, SEP and SAND\_SEP (Fig. 4a, c and e) demonstrated that the last one is smoother with lower voids. The use of sole sepiolite in combination with lime (SEP sample) determines the creation of multiple fracture lines that cause the rupture of the sample for low strength values.

Even the addition of colloidal silica (SC samples in Fig. 4b, d and f) produced a more cohesive structure than the basic samples. The combination of sepiolite with colloidal silica (SEP\_SC sample) created a jagged surface because the high pozzolanic activity of colloidal silica accelerated the hydration process

thus promoting the structure consistency and internal cohesion.

The aging (Fig. 5) had a significant effect especially for SEP samples (Fig. 5c and d), with porosity reduction as result of volume decrease for shrinkage. Furthermore, in the SEP\_SC sample, the fracture lines are even more marked than in unaged conditions.

### 4.4 Water absorption for capillarity

The results of the capillarity absorption tests are reported in Table 4. All the renders comply with the standard for thermal external applications since they all respect the threshold value ( $W < 0.4 \text{ kg/m}^2 \text{ min}^{0.5}$ ) fixed in EN 998-1. Moreover, all the sand-based formulations are also suitable for coat rendering



**Table 3** Mercury intrusion porosimetry tests measures results

	Accessible porosity (%)	Average pore diameter ( $\mu\text{m}$ )	Macropores $> 1 \mu\text{m}$ (%)	Meso pores $0.01\text{--}1 \mu\text{m}$ (%)	Micro pores $< 0.01 \mu\text{m}$ (%)
<i>At 28 days</i>					
SAND	33.8	0.22	17.3	12.8	3.7
SAND_SC	34.3	0.19	16.8	12.8	4.7
SEP	58.4	0.08	30.0	14.2	14.2
SEP_SC	60.7	0.09	31.3	15.0	14.4
SAND_SEP	36.7	0.14	23.4	8.3	5.0
SAND_SEP_SC	40.4	0.18	26.3	8.0	6.1
<i>After weathering</i>					
SAND	31.1	0.12	16.5	8.4	6.2
SAND_SC	34.3	0.10	14.5	13.4	6.4
SEP	57.1	0.08	26.1	16.8	14.2
SEP_SC	58.2	0.09	34.3	11.0	12.9
SAND_SEP	35.5	0.08	18.7	8.0	8.8
SAND_SEP_SC	36.1	0.07	18.3	6.0	11.8

mortars (class W2), having even lower water absorption values for capillarity.

Both SEP and SEP\_SC recipes showed high water sorption capabilities ( $W > 0.2 \text{ kg/m}^2 \text{ min}^{0.5}$ ), achieving class W1 and confirming the results obtained by other studies that suggested the adoption of sepiolite for evaporative cooling functions [41].

For all the samples, except for SAND\_SEP and SAND\_SEP\_SC, the aging increased the water absorption ability (Fig. 6). In unaged conditions the highest sorption rates were recorded in the samples without colloidal silica (SAND, SEP, SAND\_SEP), while after aging the porosity increase occurred in the samples with nano silica (SAND\_SC, SEP\_SC, SAND\_SEP\_SC) promoted the capillary action, with enhanced water uptake.

As clearly visible in the graph, mixed formulations comprising both sand and sepiolite, (SAND\_SEP and SAND\_SEP\_SC formulation), behaved differently by the other mixtures, demonstrating reduced water absorption after aging. This different trend could be explained by comparing the pore distribution on aged samples (Fig. 7) for one simple formulation (i.e. SAND\_SC) and one mixed formulation (i.e. SAND\_SEP\_SC). In aged SAND\_SEP\_SC samples, the pores have higher sizes than those in which capillary action typically occurs. Differently, in aged SAND\_SC

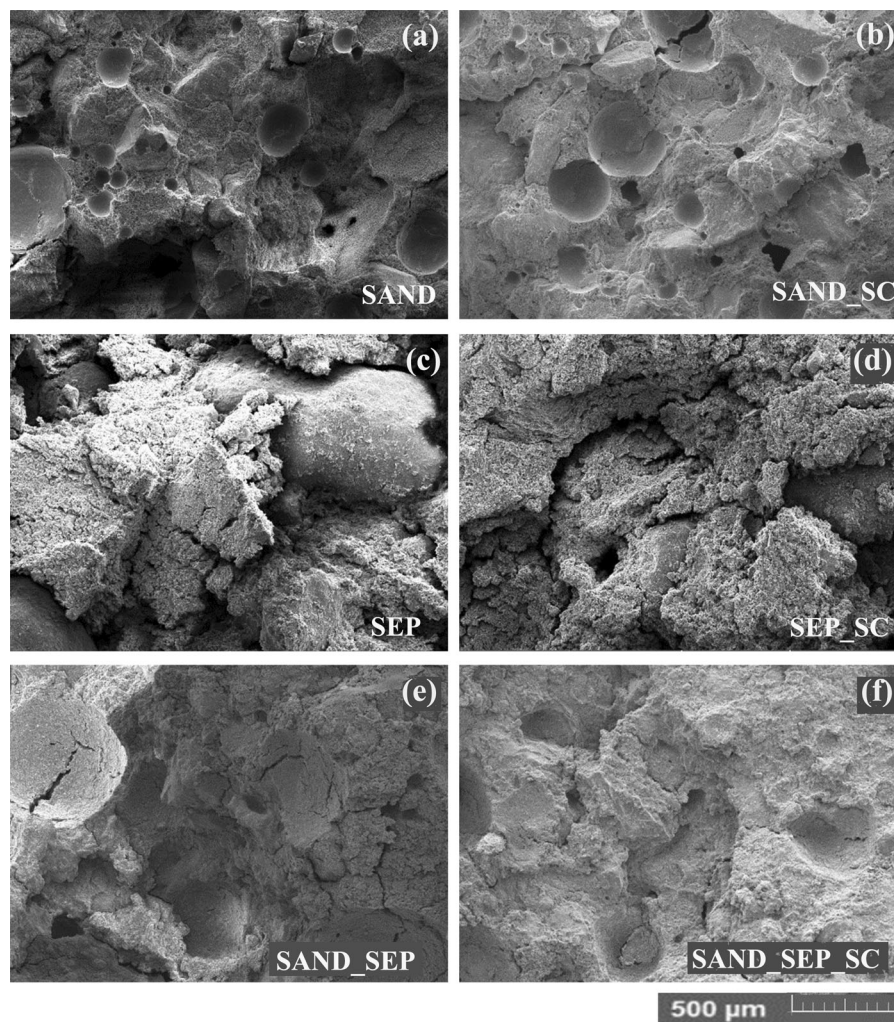
formulations, the pore sizes are more homogeneously concentrated in low-medium values, commonly characterized by capillary effect. This is also clearly visible by comparing SEM images of the two aged samples: the fracture surface in SAND\_SC is an almost smooth surface with small pores, while that of SAND\_SEP\_SC is irregular and shows larger pores.

#### 4.5 Thermal conductivity

The results of the thermal conductivity ( $\lambda$ ) tests are reported in Table 4.

The performance of sepiolite-based mortars is only slightly influenced by the presence of colloidal nano silica since they have almost the same  $\lambda$  value. Even the values of sand-based recipes are only slightly increased by nano silica additions. Most samples are classified in T2 class (T2 is for  $\lambda$  values  $\leq 0.2 \text{ W/mK}$ ). The best solutions are SEP samples, that achieve T1 class (T1 is for  $\lambda$  values  $\leq 0.1 \text{ W/mK}$ ).

The aging had not significant effect on all the formulations except for SAND\_SEP and SAND\_SEP\_SC, that showed a noticeable increase in thermal conductivity with respect to the unaged samples. The cause could be ascribed to the complexification of the internal microstructure that was subject to the reduction of pore dimensions. Moreover, a slight



**Fig. 4** SEM images of unaged samples: **a** SAND; **b** SAND\_SC; **c** SEP; **d** SEP\_SC; **e** SAND\_SEP; **f** SAND\_SEP\_SC

thermal conductivity drop was observed for the sample SEP\_SC due to the creation of macro voids as result of shrinkage and the consequent interfacial mismatch faced by the thermal wave.

#### 4.6 Mechanical performance

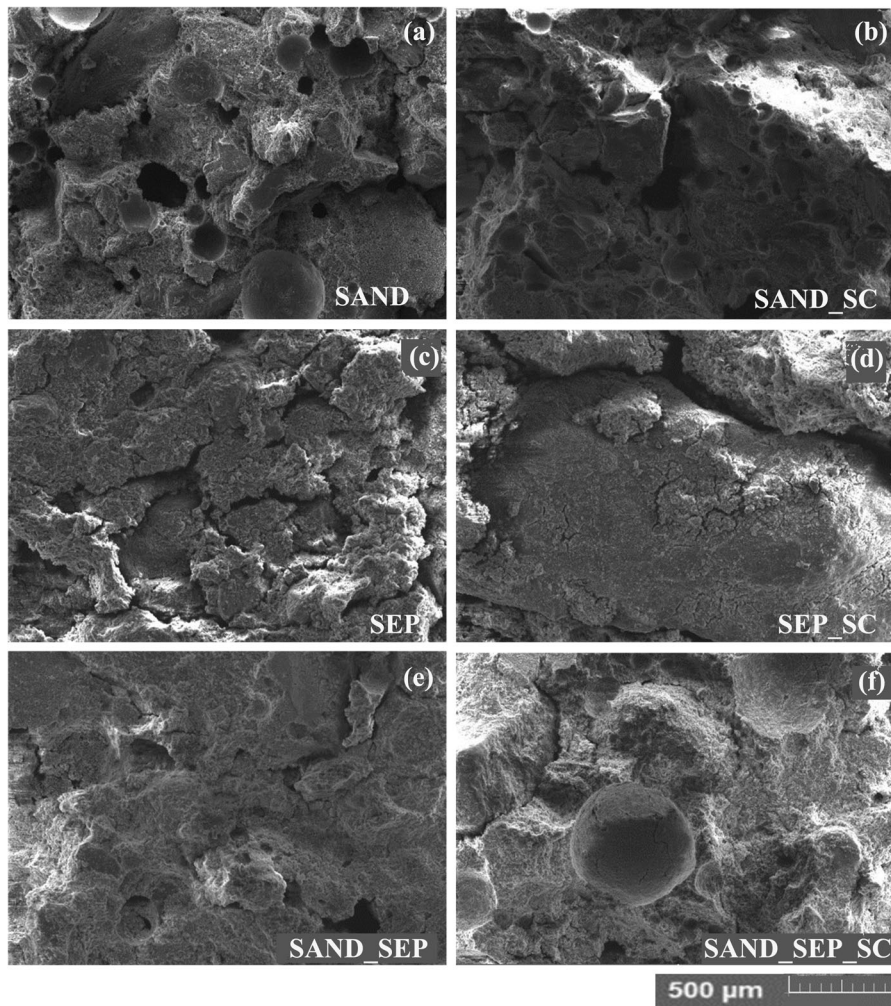
The graphs in Fig. 8a, b show the average curves obtained by the samples under compression test in aged and unaged conditions, while the histograms in Fig. 8c report the compression strength values.

As expected, the sand-based mortars, characterized by an almost doubled final bulk density respect to the other formulations, achieved the best result, with the highest compressive strength. Both sepiolite-based

renders SEP and SEP\_SC showed reduced  $\sigma_{\text{cmax}}$  values, due to the significant reduction of the recipe density.

The mixed SAND-SEP recipes (SAND\_SEP and SAND\_SEP\_SC) achieved good outcomes with high strength and enhanced ability to sustain plastic deformation under compressive stress before cracking ( $\epsilon$  up to 20%).

As regard the final strength (histograms in Fig. 8c), the aging treatment enhanced the compressive strength for almost all the formulations. This result confirms the data reported by other authors that found substantial increases in compressive strength during later curing, even if the study regarded mortars rather than renders [37, 42]. This increase in the mechanical



**Fig.5** SEM images of aged samples: **a** SAND; **b** SAND\_SC; **c** SEP; **d** SEP\_SC; **e** SAND\_SEP; **f** SAND\_SEP\_SC

properties can be attributed to the hydration of several hydraulic compounds that form hydrated calcium silicates (C-S-H phases) [43].

Differently SEP\_SC didn't increase the compressive strength, probably for the creation of an irregular structure with fractures and macro-voids, as highlighted in SEM and thermal tests.

Table 4 reports the detailed data obtained from the compression tests  $\sigma_{\text{cmax}}$  ( $\text{N/mm}^2$ ) at 28 days of curing (unaged) and after weathering cycles (aged). According to EN 998-1, the samples should be classified within the following ranges: Class CSI within  $0.4\text{--}2.5 \text{ N/mm}^2$ ; Class CSII for  $1.5\text{--}5 \text{ N/mm}^2$ ; Class CSIII for  $3.5\text{--}7.5 \text{ N/mm}^2$ ; class CSIV  $> 6 \text{ N/mm}^2$ .

The sand-based renders fall within class CSIII. Indeed, they guaranteed the highest mechanical

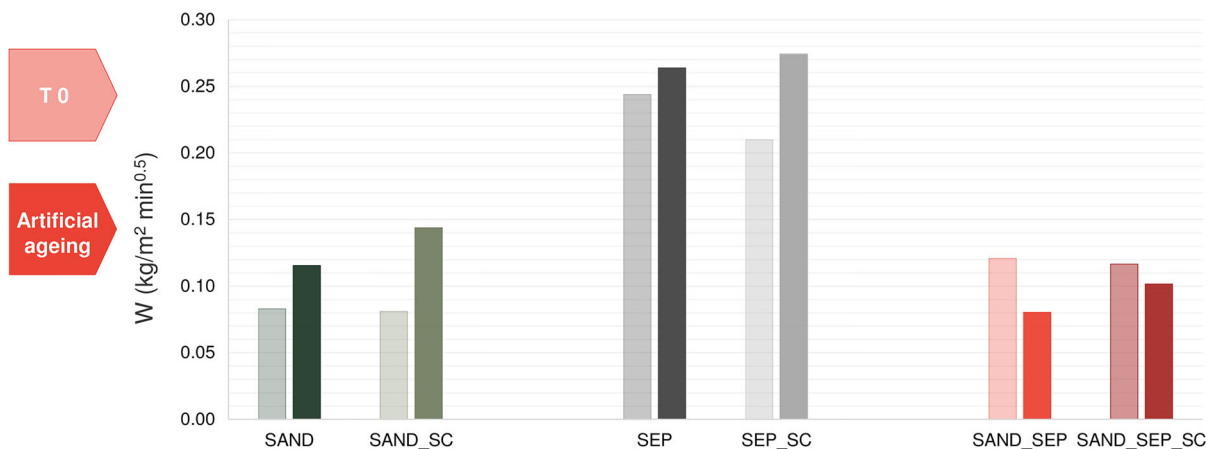
performance. The aging increased the strength class for almost all the recipes. The addition of nano silica (SC) did not contribute to the increase of the class in unaged conditions. On the contrary it reduced the final strength in almost all the formulations. Differently, in aged samples, it strongly enhanced the final performance of mixed SAND\_SEP compositions allowing the achievement of CS IV class in the SAND\_SEP\_SC sample, with benefits even in render ductility.

The graphs in Fig. 9 show the histograms with flexural strength obtained for all the samples under the three-point bending test (a), Young's modulus (b) and adhesive strength (c). The detailed data of flexural strength  $\sigma_{\text{fmax}}$  ( $\text{N/mm}^2$ ) are also reported in Table 4. As seen in the compression tests, the sand-based renders show the highest flexural performance



**Table 4** Results of the capillary absorption and thermal conductivity measurements; compression and bending test

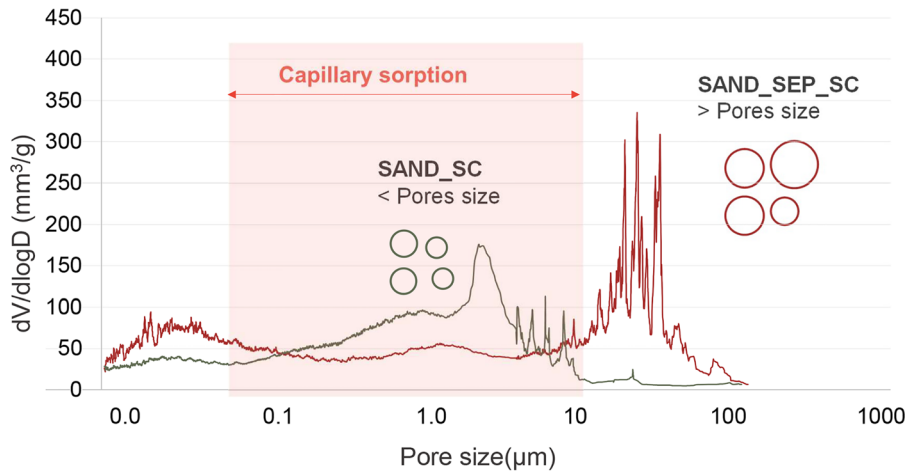
	$W$ ( $\text{kg}/\text{m}^2 \text{ min}^{0.5}$ )	$\lambda$ (W/mK)	$\sigma_{\text{cmax}}$ ( $\text{N}/\text{mm}^2$ )	$E_c$ ( $\text{N}/\text{mm}^2$ )	$\sigma_{\text{fmax}}$ ( $\text{N}/\text{mm}^2$ )	$f_{\text{u,pull off}}$ ( $\text{N}/\text{mm}^2$ )
<i>At 28 days</i>						
SAND	0.08	0.13	$5.63 \pm 0.50$	$159 \pm 48$	$1.69 \pm 0.15$	$0.11 \pm 0.01$
SAND_SC	0.08	0.17	$5.27 \pm 0.37$	172	$1.49 \pm 0.07$	$0.12 \pm 0.01$
SEP	0.24	0.07	$1.31 \pm 0.12$	$10 \pm 4$	$0.24 \pm 0.08$	$0.08 \pm 0.01$
SEP_SC	0.21	0.10	$1.10 \pm 0.08$	$14 \pm 3$	$0.33 \pm 0.46$	$0.09 \pm 0.01$
SAND_SEP	0.12	0.10	$2.35 \pm 0.21$	$103 \pm 18$	$0.87 \pm 0.08$	$0.13 \pm 0.01$
SAND_SEP_SC	0.12	0.11	$2.25 \pm 0.4$	$82 \pm 7$	$1.09 \pm 0.28$	$0.15 \pm 0.01$
<i>After weathering cycles</i>						
SAND	0.12	0.12	$8.24 \pm 0.58$	$240 \pm 31$	$2.80 \pm 0.40$	–
SAND_SC	0.14	0.18	$7.36 \pm 0.84$	$192 \pm 29$	$1.93 \pm 0.44$	–
SEP	0.26	0.07	$1.82 \pm 0.50$	$17 \pm 6$	$0.26 \pm 0.05$	–
SEP_SC	0.27	0.08	$0.81 \pm 0.20$	$9 \pm 3$	$0.88 \pm 0.20$	–
SAND_SEP	0.08	0.16	$5.28 \pm 1.20$	$111 \pm 30$	$2.07 \pm 0.56$	–
SAND_SEP_SC	0.10	0.14	$8.90 \pm 0.75$	$212 \pm 44$	$2.81 \pm 0.54$	–

**Fig. 6** Water absorption for capillarity at 28 days and after weathering cycles

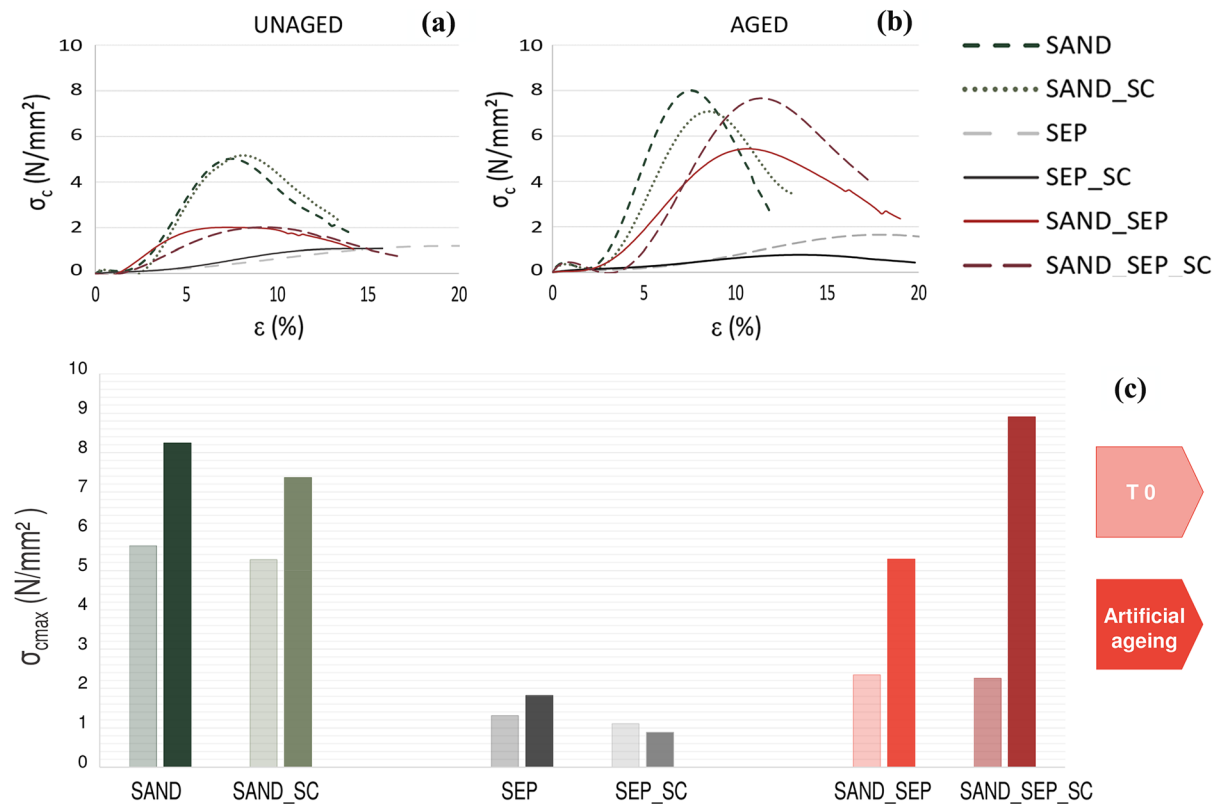
(Fig. 9a). The ageing increased the values for almost all the samples.

As regards the Young's modulus  $E_c$  ( $\text{N}/\text{mm}^2$ ) (see Table 4 and Fig. 9b), it should be as close as possible to the values recorded by the underlying support, for example an historic masonry for conservative purposes [32]. In this case the clayed support used for pull-off tests, namely an unbaked clay block masonry experimented in a previous work [44], showed a value of  $700 \text{ N}/\text{mm}^2$ , significantly higher than the values obtained by all the renders. All the renders with sand, that achieved the highest Young's modulus values,

also showed a better adhesion as demonstrated by the pull-off tests results (Fig. 9c). The modulus values are near to those obtained in works for mortars with similar compositions (i.e. [36]) while they are much lower than those obtained in other works characterized by longer service life period and variables on compositions (such as the presence of wet sand or lime putty) [44].

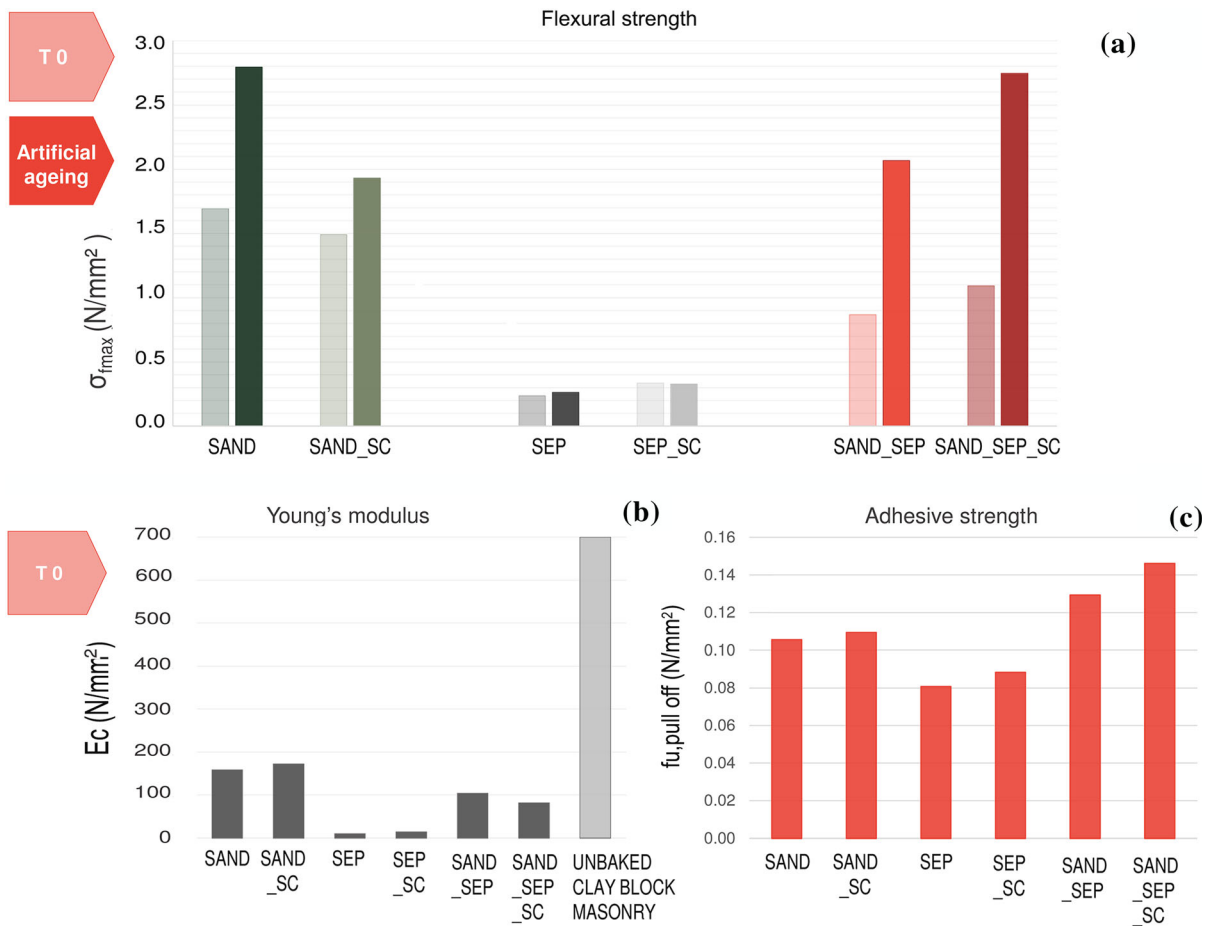


**Fig. 7** Pore distribution in aged samples: comparison between SAND\_SC and SAND\_SEP\_SC



**Fig.8 a** Stress–strain curves of the samples under axial compression at 28 days; **b** Stress–strain curves of the samples under axial compression after weathering cycles; **c** Histograms

of the compressive strength at 28 days and after weathering cycles (darker histograms)



**Fig. 9** **a** Flexural strength of the samples under three-point bending tests at 28 days and after weathering cycles; **b** Values of the Young's modulus and **c** Adhesive strength of the samples under pull off tests at 28 days of curing

## 5 Discussion

The work deepens the impact of adopting pore-modulating additives, such as sepiolite and nano silica, in lime-sand renders on water absorption, thermal and mechanical performance. Our study demonstrated that the optimal solution is different based on the considered aspect, either mechanical or thermal-hygro-metric. Figure 10 reports a summary of the performance on the multi-domain aspects considered.

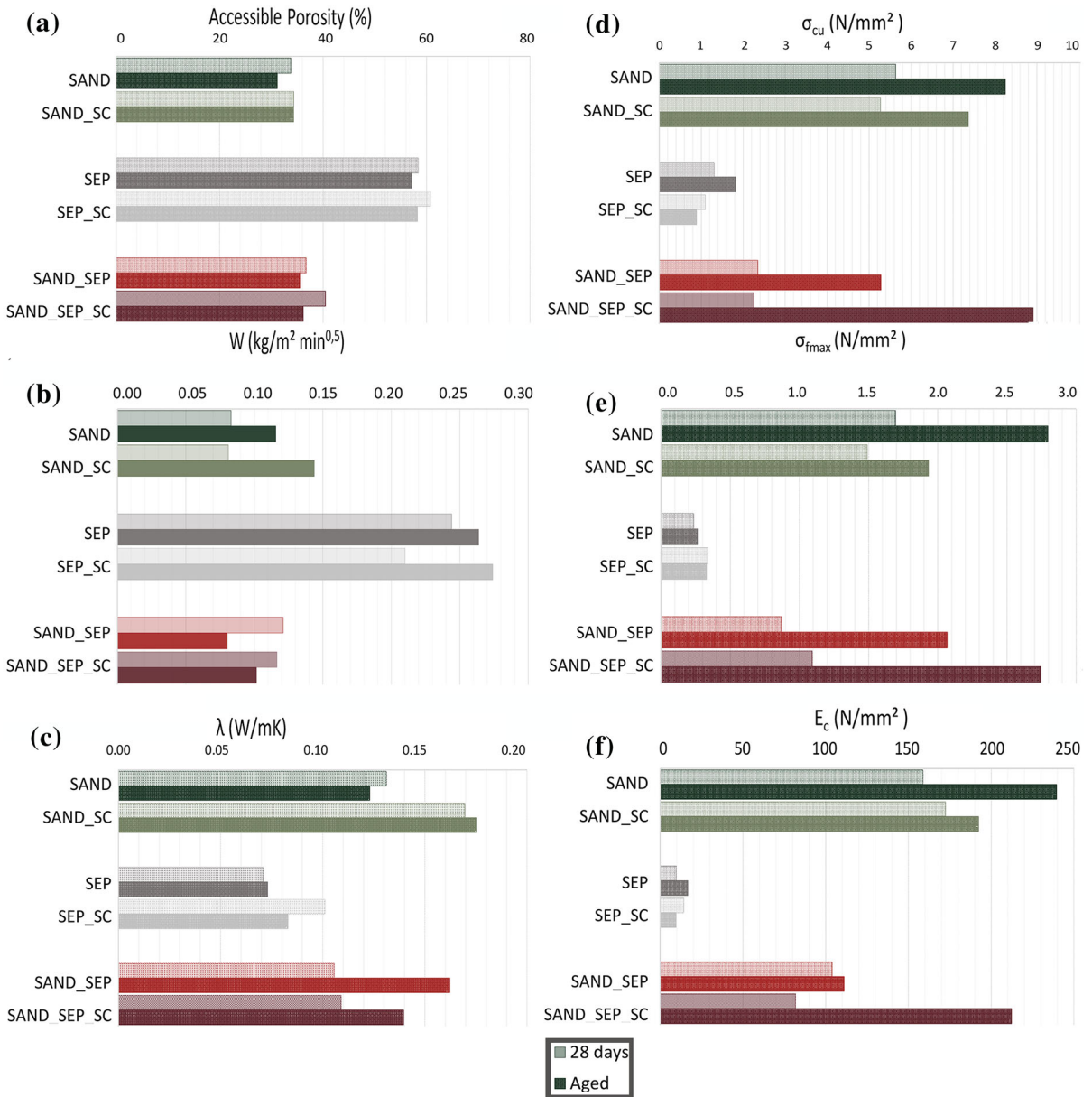
An important requirement for renders intended for wet surface uses is a good ability to adsorb water.

Indeed the hydrophilicity, rate and capacity of water vapor adsorption, are the primary factors to consider in the selection of a porous materials [41]. Capillarity is involved in the retention of fluids and it

is also very important for porous layer to be inserted in water-evaporative walls, where water will mainly be absorbed by capillarity [13]. In this regard, the test on water uptake by capillarity shows that the renders with sepiolite (SEP samples), thanks to their greatest accessible porosity (Fig. 10a), have the highest performance (Fig. 10b).

Another aspect to consider for the selection of appropriate finishing materials in high urban temperatures is that the mitigation of overheating requires the use of low thermal-conductivity building materials [45, 46] since they may heat up at the surface but will not transfer the heat throughout the layers behind the surface as quickly as those with higher conductivity. Both the renders with sepiolite additions (SEP and SEP\_SC) show the lowest thermal conductivity values (Fig. 10c).





**Fig.10** Summary of multidomain performance of the samples at 28 days and after weathering cycles (darker histograms): **a** accessible porosity; **b** water absorption; **c** thermal conductivity; **d** compressive strength; **e** flexural strength; **f** Young's modulus

As regards the resolution of possible shrinkage problems and the improvement of mechanical stability, the sand substitution with sepiolite has the effect of both compressive and flexural strength reduction (Fig. 10d, e). The minimum values recommended by DIN18974 for earth render are 1 MPa in compression and 0.3 MPa under bending stress. Such limits are not reached by the render with sepiolite. The addition of

colloidal nano silica increases the flexural strength but has an inverse effect on the compressive strength.

For the mechanical aspects in general the sand-based solutions (both simple and mixed formulations) achieved the best results. The addition of sepiolite on cement composite was found in literature to increase both the compressive and bending strengths [19] through the modification of the rheological properties

of the cement mortar. However, several authors agreed that the adoption of small size sand achieves worst performance than mix of medium sized and fine aggregates. This can explain the low strength observed here in the sepiolite-based renders since selected sepiolite powder has lower dimension than sand used in the reference render. Even other authors [32], found that lime/sand mortars (in the ratio 1:3) as in the present work, reached a very low bending strength because of the very fine sand (maximum diameter of 0.8 mm) used in the samples, which did not provide enough structure to the render.

The use of mixed SAND\_SEP\_SC formulations, especially after aging, seem to behave similarly to simple sand-based solutions as regards the mechanical aspects, with high compressive strength, bending strength and elastic modulus (Fig. 10d, e and f). These formulations, in service life conditions (after aging), showed also increased porosity and similar water absorption and thermal performance respect to pure sand samples. So, the adoption of such more complex formulations doesn't worth the cost for the reduced benefit presented.

The aging caused the worsening of the thermal behavior of almost all the recipes while significantly improved their mechanical performance, confirming other authors results [18]. The greatest effect of ageing was recorded by the mixed SAND\_SEP\_SC recipes that showed a noticeable mechanical performance increase.

While these findings could be of interest for appropriate render selection, the present study had some limitations. Indeed only 6 mixes were studied and only a single test period was considered after aging, so that the evolution of properties on the long term was not addressed. Moreover, the cooling effect due to water adsorption and subsequent evaporation is surely good in the hot season but it could decrease the thermal insulation during the cold period. Future studies should consider these aspects. Moreover, for very capillary mortars, such as lime-based mortars, it would be interesting to deepen the aspects connected to evaporative cooling functionalities (through evaporation experiments and water vapor retention) and the possible saturation in the initial phase of the capillary absorption through specific tests.

## 6 Conclusions

The present work was aimed at identifying the effect of the use of sepiolite and colloidal nanosilica in lime renders on their workability, physical, thermal, and mechanical performance even after aging.

The results of the investigations allowed to conclude that:

- Sepiolite powder can be successfully incorporated into hydraulic lime recipes in substitution of sand, thanks to enhanced sorption ability, medium-low thermal conductivity, and low thermal capacity. However, the mechanical performance resulted very low.
- The use of colloidal nano silica in combination with the pure sepiolite was unsuccessful in resolve this drawback, not verifying the enhancement of the mechanical behavior.
- Mixed solutions with sand, sepiolite and nano silica behave similarly to the recipe with pure sand demonstrating that the behavior is mainly governed by the presence of sand.

In summary it can be concluded that the addition of sand has the major impact on the properties of the lime renders. The use of sepiolite has the effect of lowering the mechanical property values and increasing the water absorption ability. The addition of nano-silica has only limited effects on the mechanical properties. The weathering has a great effect on the modification of sample properties with a noticeable increase in the mechanical performance.

**Open Access** This article is licensed under a Creative Commons Attribution 4.0 International License, which permits use, sharing, adaptation, distribution and reproduction in any medium or format, as long as you give appropriate credit to the original author(s) and the source, provide a link to the Creative Commons licence, and indicate if changes were made. The images or other third party material in this article are included in the article's Creative Commons licence, unless indicated otherwise in a credit line to the material. If material is not included in the article's Creative Commons licence and your intended use is not permitted by statutory regulation or exceeds the permitted use, you will need to obtain permission directly from the copyright holder. To view a copy of this licence, visit <http://creativecommons.org/licenses/by/4.0/>.



## References

- Rahman T, Nagano K, Togawa J (2019) Study on building surface and indoor temperature reducing effect of the natural meso-porous material to moderate the indoor thermal environment. *Energy Build* 191:59–71. <https://doi.org/10.1016/j.enbuild.2019.03.014>
- Smith DS et al (2013) Thermal conductivity of porous materials. *J Mater Res* 28(17):2260–2272. <https://doi.org/10.1557/jmr.2013.179>
- Chan HY, Riffat SB, Zhu J (2010) Review of passive solar heating and cooling technologies. *Renew Sustain Energy Rev* 14(2):781–789. <https://doi.org/10.1016/j.rser.2009.10.030>
- He J, Hoyano A (2010) Experimental study of cooling effects of a passive evaporative cooling wall constructed of porous ceramics with high water soaking-up ability. *Build Environ* 45(2):461–472. <https://doi.org/10.1016/j.buildenv.2009.07.002>
- Karamanis D, Kyritsi E, Krimpali S (2015) Well-ordered nanoporous materials for low-temperature water phase changes and solar evaporative cooling. *Sol Energy Mater Sol Cells* 139:34–43. <https://doi.org/10.1016/j.solmat.2015.03.013>
- Kandya A, Mohan M (2018) Mitigating the Urban Heat Island effect through building envelope modifications. *Energy Build* 164:266–277. <https://doi.org/10.1016/j.enbuild.2018.01.014>
- Karamanis D, Vardoulakis E, Kyritsi E, Ökte N (2012) Surface solar cooling through water vapor desorption from photo-responsive sepiolite nanocomposites. *Energy Convers Manag* 63:118–122. <https://doi.org/10.1016/j.enconman.2012.01.035>
- Andrejkovičová S, Ferraz E, Velosa AL, Silva AS, Rocha F (2012) Air lime mortars with incorporation of sepiolite and synthetic zeolite pellets. *Acta Geodyn Geomater* 9(1):79–91
- Sepulcre-Aguilar A, Hernández-Olivares F (2010) Assessment of phase formation in lime-based mortars with added metakaolin, Portland cement and sepiolite, for grouting of historic masonry. *Cem Concr Res* 40(1):66–76. <https://doi.org/10.1016/j.cemconres.2009.08.028>
- González JC, Molina-Sabio M, Rodríguez-Reinoso F (2001) Sepiolite-based adsorbents as humidity controller. *Appl Clay Sci* 20(3):111–118. [https://doi.org/10.1016/S0169-1317\(01\)00062-X](https://doi.org/10.1016/S0169-1317(01)00062-X)
- Di Giuseppe E, Drazio M (2014) Moisture buffering ‘active’ devices for indoor humidity control: preliminary experimental evaluations. *Energy Procedia* 62:42–51. <https://doi.org/10.1016/j.egypro.2014.12.365>
- Wu Y, Gong G, Yu CWF, Fang P (2014) The hygroscopic properties of wood fibre, sepiolite and expanded perlite-based breathable wall for moderating the humidity environment. *Indoor Built Environ* 23(2):299–312. <https://doi.org/10.1177/1420326X13505105>
- Naticchia B, D’Orazio M, Carbonari A, Persico I (2010) Energy performance evaluation of a novel evaporative cooling technique. *Energy Build* 42(10):1926–1938. <https://doi.org/10.1016/j.enbuild.2010.05.029>
- Zhang Y, Zhang L, Meng Q, Feng Y, Chen Y (2017) A dynamic experimental study on the evaporative cooling performance of porous building materials. *Heat Mass Transf* 53:2651–2662. <https://doi.org/10.1007/s00231-017-2009-4>
- Černý R, Kunca A, Tydlitát V, Drchalová J, Rovnaníková P (2006) Effect of pozzolanic admixtures on mechanical, thermal and hygric properties of lime plasters. *Constr Build Mater* 20(10):849–857. <https://doi.org/10.1016/j.conbuildmat.2005.07.002>
- Corinaldesi V, Mazzoli A, Moriconi G (2011) Mechanical behaviour and thermal conductivity of mortars containing waste rubber particles. *Mater Des* 32(3):1646–1650. <https://doi.org/10.1016/j.matdes.2010.10.013>
- Westgate P, Paine K, Ball RJ (2018) Physical and mechanical properties of plasters incorporating aerogel granules and polypropylene monofilament fibres. *Constr Build Mater* 158:472–480. <https://doi.org/10.1016/j.conbuildmat.2017.09.177>
- Andrejkovičová S, Ferraz E, Velosa AL, Silva AS, Rocha F (2011) Fine sepiolite addition to air lime-metakaolin mortars. *Clay Miner* 46(4):621–635. <https://doi.org/10.1180/claymin.2011.046.4.621>
- Kavas T, Sabah E, Çelik MS (2004) Structural properties of sepiolite-reinforced cement composite. *Cem Concr Res* 34(11):2135–2139. <https://doi.org/10.1016/j.cemconres.2004.03.015>
- Canbaz M, Eryilmaz M (2016) Effect of high temperature on sepiolite-hydraulic lime mortar. *Int Conf Perform-based Life-cycle Struc Eng*. <https://doi.org/10.14264/uql.2016.543>
- Du H, Pang SD (2019) High performance cement composites with colloidal nano-silica. *Constr Build Mater* 224:317–325. <https://doi.org/10.1016/j.conbuildmat.2019.07.045>
- Nazari A, Riahi S (2011) The role of SiO<sub>2</sub> nanoparticles and ground granulated blast furnace slag admixtures on physical, thermal and mechanical properties of self compacting concrete. *Mater Sci Eng A* 528(4–5):2149–2157. <https://doi.org/10.1016/j.msea.2010.11.064>
- Ying J, Zhou B, Xiao J (2017) Pore structure and chloride diffusivity of recycled aggregate concrete with nano-SiO<sub>2</sub> and nano-TiO<sub>2</sub>. *Constr Build Mater* 150:49–55. <https://doi.org/10.1016/j.conbuildmat.2017.05.168>
- Prashanth R, Senthil Selvan S, Balasubramanian M (2019) Experimental investigation on durability properties of concrete added with nano silica. *Rasayan J Chem* 12(2):685–690. <https://doi.org/10.31788/RJC.2019.1225165>
- Tobón JI, Payá J, Restrepo OJ (2015) Study of durability of Portland cement mortars blended with silica nanoparticles. *Constr Build Mater* 80:92–97. <https://doi.org/10.1016/j.conbuildmat.2014.12.074>
- Jalal M, Mansouri E, Sharifipour M, Pouladkhan AR (2012) Mechanical, rheological, durability and microstructural properties of high performance self-compacting concrete containing SiO<sub>2</sub> micro and nanoparticles. *Mater Des* 34:389–400. <https://doi.org/10.1016/j.matdes.2011.08.037>
- Du H, Du S, Liu X (2014) Durability performances of concrete with nano-silica. *Constr Build Mater* 73:705–712. <https://doi.org/10.1016/j.conbuildmat.2014.10.014>
- Facconi L, Conforti A, Minelli F, Plizzari GA (2015) Improving shear strength of unreinforced masonry walls by



- nano-reinforced fibrous mortar coating. *Mater Struct* 48:2557–2574. <https://doi.org/10.1617/s11527-014-0337-0>
29. van Hees R, Veiga R, Slížková Z (2017) Consolidation of renders and plasters. *Mater Struct*. <https://doi.org/10.1617/s11527-016-0894-5>
30. Válek J, Hughes JJ, Pique F, Gulotta D, van Hees R, Papayiani I (2019) “Recommendation of RILEM TC 243-SGM: functional requirements for surface repair mortars for historic buildings. *Mater Struct*. <https://doi.org/10.1617/s11527-018-1284-y>
31. Elert K, Rodriguez-Navarro C, Pardo ES, Hansen E, Cazalla O (2002) Lime mortars for the conservation of historic buildings. *Stud Conserv* 47(1):62–75. <https://doi.org/10.1179/sic.2002.47.1.62>
32. Hamard E, Morel JC, Salgado F, Marcom A, Meunier N (2013) A procedure to assess the suitability of plaster to protect vernacular earthen architecture. *J Cult Herit* 14(2):109–115. <https://doi.org/10.1016/j.culher.2012.04.005>
33. Stazi F, Nacci A, Tittarelli F, Pasqualini E, Munafò P (2016) An experimental study on earth plasters for earthen building protection: the effects of different admixtures and surface treatments. *J Cult Herit* 17:27–41. <https://doi.org/10.1016/j.culher.2015.07.009>
34. Mukharjee B, Barai SV (2014) Characteristics of mortars containing colloidal nano-silica. *Int J Appl Eng Res* 9(1):17–22
35. Wu Y, Gong G, Yu CW, Huang Z (2015) Proposing ultimate moisture buffering value (UMBV) for characterization of composite porous mortars. *Constr Build Mater* 82:81–88. <https://doi.org/10.1016/j.conbuildmat.2015.02.058>
36. Middendorf B, Hughes JJ, Callebaut K, Baronio G, Papayanni I (2005) Investigative methods for the characterisation of historic mortars—part 1: mineralogical characterisation. *Mater Struct* 38:761–769. <https://doi.org/10.1617/14281>
37. Costigan A, Pavia S, Kinnane O (2015) An experimental evaluation of prediction models for the mechanical behavior of unreinforced, lime-mortar masonry under compression. *J Build Eng* 4:283–294. <https://doi.org/10.1016/j.jobbe.2015.10.001>
38. Enea D, Bellardita M, Scalisi P, Alaimo G, Palmisano L (2019) Effects of weathering on the performance of self-cleaning photocatalytic paints. *Cement Concr Compos* 96:77–86. <https://doi.org/10.1016/j.cemconcomp.2018.11.013>
39. Al-Akhras N, Ababneh A, Alaraji WA (2010) Using burnt stone slurry in mortar mixes. *Constr Build Mater* 24(12):2658–2663. <https://doi.org/10.1016/j.conbuildmat.2010.04.058>
40. Abd El Aleem S, Heikal M, Morsi WM (2014) Hydration characteristic, thermal expansion and microstructure of cement containing nano-silica. *Constr Build Mater* 59:151–160. <https://doi.org/10.1016/j.conbuildmat.2014.02.039>
41. Karamanis D, Ökte AN, Vardoulakis E, Vaimakis T (2011) Water vapor adsorption and photocatalytic pollutant degradation with TiO<sub>2</sub>-sepiolite nanocomposites. *Appl Clay Sci* 53(2):181–187. <https://doi.org/10.1016/j.clay.2010.12.012>
42. Garijo L, Zhang X, Ruiz G, Ortega JJ (2020) Age effect on the mechanical properties of natural hydraulic and aerial lime mortars. *Constr Build Mater* 236:117573. <https://doi.org/10.1016/j.conbuildmat.2019.117573>
43. Lanás J, Bernal JLP, Bello MA, Galindo JIA (2004) Mechanical properties of natural hydraulic lime-based mortars. *Cem Concr Res* 34(12):2191–2201. <https://doi.org/10.1016/j.cemconres.2004.02.005>
44. Stazi F, Serpilli M, Chiappini G, Pergolini M, Fratolocchi E, Lenci S (2020) Experimental study of the mechanical behaviour of a new extruded earth block masonry. *Constr Build Mater* 244:118368. <https://doi.org/10.1016/j.conbuildmat.2020.118368>
45. Elsayed ISM (2012) Elsayed, “Mitigation of the urban heat island of the city of Kuala Lumpur, Malaysia.” *Middle East J Sci Res* 11:1602–1613. <https://doi.org/10.5829/idosi.mejsr.2012.11.11.1590>
46. Kakoniti A, Georgiou G, Marakkos K, Kumar P, Neophytou MKA (2016) The role of materials selection in the urban heat island effect in dry mid-latitude climates. *Environ Fluid Mech* 16:347–371. <https://doi.org/10.1007/s10652-015-9426-z>

**Publisher’s Note** Springer Nature remains neutral with regard to jurisdictional claims in published maps and institutional affiliations.

